Environ. Sci. Technol. **2004**, *38,* 5101−5111

Macroscopic and Microscopic Observations of Particle-Facilitated Mercury Transport from New Idria and Sulphur Bank Mercury Mine Tailings

GREGORY V. LOWRY,[†,||] SAMUEL SHAW,*[,†,⊥] CHRISTOPHER S. KIM,[†,○] JAMES J. RYTUBA,[‡] AND GORDON E. BROWN, JR.[†,§]

Surface and Aqueous Geochemistry Group, Department of Geological and Environmental Sciences, Stanford University, Stanford, California 94305-2115, U.S. Geological Survey, 345 Middlefield Road, MS 901, Menlo Park, California 94025, and Stanford Synchrotron Radiation Laboratory, SLAC, 2575 Sand Hill Road, MS 99, Menlo Park, California 94025

Mercury (Hg) release from inoperative Hg mines in the California Coast Range has been documented, but little is known about the release and transport mechanisms. In this study, tailings from Hg mines located in different geologic settings—New Idria (NI), a Si-carbonate Hg deposit, and Sulphur Bank (SB), a hot-spring Hg deposit—were characterized, and particle release from these wastes was studied in column experiments to (1) investigate the mechanisms of Hg release from NI and SB mine wastes, (2) determine the speciation of particle-bound Hg released from the mine wastes, and (3) determine the effect of calcinations on Hg release processes. The physical and chemical properties of tailings and the colloids released from them were determined using chemical analyses, selective chemical extractions, XRD, SEM, TEM, and X-ray absorption spectroscopy techniques. The total Hg concentration in tailings increased with decreasing particle size in NI and SB calcines (roasted ore), but reached a maximum at an intermediate particle size in the SB waste rock (unroasted ore). Hg in the tailings exists predominantly as low-solubility HgS (cinnabar and metacinnabar), with NI calcines having >50% HgS, SB calcines having >89% HgS, and SB waste rock having ∼100% HgS. Leaching experiments with a high-ionic-strength solution (0.1 M NaCl) resulted in a rapid but brief release of soluble and particulate Hg. Lowering the ionic strength of the leach solution (0.005 M NaCl) resulted in the release of colloidal Hg from two of the three mine wastes studied (NI calcines and SB waste rock). Colloid-associated Hg accounts for as much as 95% of the Hg released during episodic particle release. Colloids generated from the NI calcines are produced by a breakup and release mechanism and consist of hematite, jarosite/alunite, and Al−Si gel with particle sizes of 10−200 nm. ATEM and XAFS analyses indicate that the majority (∼78%) of the mercury is present in the form of HgS. SB calcines also produced HgS colloids. The colloids generated from the SB waste rock were heterogeneous and varied in composition according to the column influent composition. ATEM and XAFS results indicate that Hg is entirely in the HgS form. Data from this study identify colloidal HgS as the dominant transported form of Hg from these mine waste materials.

Introduction

The colloid-facilitated transport of heavy metal contaminants has been implicated in a number of studies (*1*−*7*). In particular, field studies have shown that Hg associated with particulate material may be an important vector for Hg migration from abandoned Hg mine sites in California (*8*, *9*). Despite this work, little is known about the mechanisms of colloid formation at Hg contaminated land sites and the speciation of Hg associated with the particles. Differences in the mineralogy and pore water chemistry in the mine tailings can significantly influence the extent of colloid release (*10*), therefore the potential for particulate facilitated transport may be dependent on the type of Hg ore deposits (e.g., silica-carbonate vs hot spring) mined and the nature of the ore extraction processes used (e.g., calcinations) (*11*). Distinguishing between particulate (colloidal) and dissolved Hg is important because the speciation can affect bioavailability and subsequent methylation (*12*, *13*). For example, Farrell et al. (*14*) observed a pronounced inhibition in Hg methylation rate by microbes when Hg was associated with mineral colloidal particles and found that the degree of inhibition was influenced by the mineralogy of the colloidal phase.

Mobile colloids released from the surfaces of the aquifer matrix have been observed in natural groundwater (*3*, *5*, *15*), with colloid release often occurring as a result of changes in the chemical composition of the pore water (*16*−*19*). Particle release and transport are often studied in laboratory soil−water columns where particle release is initiated by a chemical perturbation such as a step decrease in ionic strength (*17*−*22*). These types of experiments are useful for investigating the colloid release rate and the formation mechanism and speciation of contaminants associated with the particulates (*1*, *10*, *16*, *19*, *23*−*25*). For mine wastes these types of experiments are particularly relevant because ionic strength or pH fronts due to seasonal variations in rainfall are likely to move through tailings piles, and may lead to particle release (*8*).

The California Coast Range contains over 70 abandoned Hg mine sites which have had ore extracted from both silica-carbonate type and hot-spring type ore deposits. This study has investigated the particulate facilitated transport of Hg from the New Idria (NI) and Sulphur Bank (SB) mines situated within the mountain range. Brief descriptions of mines and ore deposits are provided to highlight important differences between them. Additional information about the Hg mines in the NI and SB mining districts, including a detailed description of each ore deposit, are given elsewhere (*8*, *9*, *26*−*28*). The NI Hg mine lies in the southern Diablo Range of the California Coast Range in central California (San Benito

* Corresponding author e-mail: Sam.Shaw@earth.ox.ac.uk.
† Stanford University.
‡ U.S. Geological Survey.
§ Stanford Synchrotron Radiation Laboratory.
|| Present address: Department of Civil & Environmental Engineering, Carnegie Mellon University, Pittsburgh, Pennsylvania 15213-3890.
⊥ Present address: Department of Earth Sciences, University of Oxford, Parks Road, Oxford, OX1 3PR, UK.
○ Present address: Department of Physical Sciences, Chapman University, Orange, CA 92866.

10.1021/es034636c CCC: $27.50
Published on Web 08/31/2004

TABLE 1. Primary Mineralogy and Hg Speciation in Select New Idria and Sulphur Bank Mercury Mine Wastes

particle size (μm)	New Idria (calcines) (processed)	Sulphur Bank (calcines) (processed)	Sulphur Bank (waste rock) (unprocessed)
	XRD Identifiable Matrix Components		
all sizes	quartz, alunite-jarosite, hematite, illite, K-feldspar	quartz, hematite, montmorillonite, cristobalite, plagioclase feldspar	cristobalite, anatase (TiO_2), cinnabar, mackinawite (FeS), quartz
	EXAFS Identifiable Hg Minerals		
$2000 > d_p > 500$	56%[a] Hg-sulfides 22% HgO 22% $Hg_3Cl_3O_2H$	89% Hg-sulfides 11% $HgCl_2$	100% Hg-sulfides
$125 > d_p > 75$	69% Hg-sulfides 31% HgO	100% Hg-sulfides	100% Hg-sulfides
$d_p < 45$	48% Hg-sulfides 21% $Hg_3S_2Cl_2$ 16% HgO 15% $Hg_3Cl_3O_2H$	100% Hg-sulfides	100% Hg-sulfides

[a] All values ±10% based on previous studies using model compounds (*29*).

Co., CA). Hg exists in a silica (SiO_2, amorphous)-carbonate ($FeCO_3$, $MgCO_3$)-type deposit present at the point of contact between the Panoche shales and a serpentine body. The Hg ore occurs in veins at the contact between these two rock types, primarily as Hg-sulfides (cinnabar and metacinnabar) and elemental mercury with secondary Hg-sulfates, -chlorides, and -oxides. The SB Hg mine lies at the northern end of the California Coast Range Hg mining belt (Lake Co., CA). The ore body is a hot-spring deposit situated in a clastic aluminosilicate host rock consisting of feldspar, quartz, and clays. Hg is present primarily as Hg-sulfides (cinnabar) with secondary Hg-sulfates, -chlorides, and -(oxy)chlorates.

In this study we have used chemical, microscopic, spectroscopic, and diffraction techniques to characterize the mineralogy, chemistry, and Hg speciation, on the macro- and microscopic scales, in NI and SB mine tailings. Following this we have used laboratory column experiments to initiate particle release from the tailings to investigate the kinetics and mechanism of colloid release and to characterize the speciation of Hg associated with the suspended particles. The main goal is to link composition and physical characteristics (e.g., particle size distribution) of the mine tailings to the formation mechanism and composition of the colloids released from these contaminated sediments to better understand the release and transport mechanisms of Hg from these mine sites. The specific objectives are to (1) investigate the mechanisms of Hg release from NI and SB mine wastes, (2) determine the speciation of particle-bound Hg released from the mine wastes, and (3) determine the effect of calcinations on Hg release processes.

Materials and Methods

Mine Tailing Sample Collection and Characterization. Mine tailings consisting of calcines and waste rock were collected from the NI and SB Hg mines. Calcines are processed ore materials that have been heated to ~700 °C to remove Hg, and the waste rock is unprocessed tailings considered to be too low in Hg for economical recovery. The top several cm of material was removed and approximately 2 kg of each material (composite) was collected. Three samples were used for this study; calcines from the NI mine tailings, calcines from the SB mine, and waste rock from the SB mine. Samples were oven dried at 105 °C for 24 h and then dry sieved into different size fractions using a Rotap to facilitate particle separation (see Table 1). Particles in the range $500\ \mu m < d_p < 2000\ \mu m$ were used in column studies and particles with $d_p < 45\ \mu m$ were used for TEM analysis. It should be noted that dry sieving likely provided incomplete sample fractionation such that small particles adhering to the surfaces of larger particles were not completely removed. It must also be noted that oven drying the calcines at 105 °C did not significantly affect the mineralogy of the calcines as they had been previously exposed to high temperatures (~700 °C) during roasting, but oven drying most natural samples prior to analysis is not recommended as this can significantly alter the temperature-sensitive minerals present in samples.

Total Hg ($[Hg]_T$) in each size fraction was determined by dissolving the samples in aqua regia followed by analysis using cold vapor atomic fluorescence spectroscopy (CVAFS) according to EPA method 1631. Al, Fe, and P concentrations of each sieve fraction were determined using inductively coupled plasma-atomic emission spectrometry (ICP-AES) according to EPA method 200.7 after aqua regia digestion. The bulk mineralogy of each tailing size fraction was determined by powder X-ray diffraction (XRD) using a Rigaku Geigerflex diffractometer.

The speciation of Hg in three size fractions of the NI and SB tailings ($5000\ \mu m < d_p < 2000\ \mu m$, $75\ \mu m < d_p < 125\ \mu m$, and $d_p < 45 \mu m$), and in colloids released in the column experiments was determined using EXAFS spectroscopy and selective sequential chemical extractions. The EXAFS analysis was performed by linear least-squares fitting of the unknown spectrum to Hg L_{III} EXAFS spectra from a Hg model compound spectral library following the method of Kim et al. (*29*). To determine the speciation of Hg associated with the coprecipitated $Hg(NO_3)_2$/SB calcine column effluent colloids, the Hg L_{III}-EXAFS data were analyzed using EXAFSPAK following the method of Kim et al. (*30*, *31*). Selective sequential extraction analyses were conducted on the $2000\ \mu m < d_p < 500\ \mu m$ sieved size fractions of pre- and postcolumn samples for each waste by Frontier Geosciences (Seattle, WA) using previously developed protocols (*32*). Samples were exposed to a series of six extraction steps of increasing intensity (see Table 2). Each extract was analyzed for $[Hg]_T$ according to EPA Method 1631. A similar series of sequential chemical extractions were performed on the colloids collected from NI calcines. The colloidal suspensions were dialyzed for 3 days in deionized water and then freeze-dried. A 0.2-g sample of dried powder was then leached using the steps used for the mine tailing, but with steps F1, F2, and F6 removed. F1 was removed because the particles were suspended in water in the column and F6 was removed because, due to the fine grained nature of the sample, any HgS would be completely dissolved by aqua regia.

The mine tailings and colloidal particles released during the column experiments were characterized using a JEOL 5600 scanning electron microscope (SEM) equipped with an energy dispersive X-ray (EDX) detector and a JEOL 200CX

TABLE 2. Sequential Chemical Extraction Method for Determining Hg Speciation as Developed by Bloom and Katon (*46*), Including Extraction Steps, the General Category of Hg Phases Removed in Each Step, and Specific Hg Compounds Typically Removed in Each Step

step	extractant	description	Hg (wt %) extracted from NI colloids	typical compounds removed
F1	DI water	water soluble	NA	$HgCl_2$
F2	pH 2 HCl/HOAc	"stomach acid"	NA	HgO, $HgSO_4$
F2m[a]	1 N HNO_3	similar to F2	33	
F3	1 N KOH	organo-complexed	1	Hg-humics, Hg_2Cl_2, CH_3Hg
F4	12 N HNO_3	strong complexed	50	mineral lattice, Hg_2Cl_2, Hg°
F5	aqua regia	Hg-sulfides	16	HgS, HgSe
F6	10:5:2 HNO_3/HF/HCl	complete dissolution	NA	residual Hg

[a] Modified extraction step for Hg speciation in colloids generated from NI tailings.

transmission electron microscope (TEM) operated at 200 kV and equipped with a Kevex high angle EDX detector.

Column Experiments. Chromatographic columns (water-saturated) filled with tailings were used to study particle release and transport (*1*, *10*, *16*, *23*). Particle release from NI calcines, SB calcines, and SB waste rock was facilitated using systematic variations in the ionic strength of the column influent solution using the following procedure. A 25-mm (i.d.) by 500-mm glass chromatographic column was dry packed with calcines or waste rock (2000 μm > d_p > 500 μm size fraction) and purged with carbon dioxide at 10 psi for approximately 1 h to displace the air in the column. Column influent solutions were delivered in an upflow configuration at lab temperature (20−24 °C). To provide stable and uniform initial conditions for each mine waste (i.e., only Na cations adsorbed), the columns were preconditioned by flowing ∼100−200 pore volumes of a high-ionic-strength electrolyte solution (0.1 M NaCl) through the column. This ionic strength is similar to that found in mine drainage at these sites at the first rainfall (*8*), and has been used in previous studies (*1*). In addition to the NaCl, malonic acid (15 mM) was added to enhance colloid release such that enough material could be collected to study; sodium azide (1 mM) was present to inhibit microbial growth; and finally NaOH was added until pH = 5.6−5.8 was attained. After preconditioning, a lower ionic strength solution (0.005 M NaCl) was flowed through the column to initiate particle release. For the NI (NI1) calcines an initial column experiment was run on the mine tailing as described above, but with no malonic acid. This was followed immediately by preconditioning and particle release steps with malonic acid present. Also, a second experiment run was performed on another sample of the NI calcines (NI2) with the same conditions (malonic acid present) as described above, but with a larger drop in ionic strength (0.5 to 0.02 M NaCl) to assess, qualitatively, the amount of colloids released as a function of the ionic strength drop. The physical parameters (porosity, pore volume, and mass of tailings) and influent chemical conditions for each step (preconditioning and particle release) for each column are given in the Supporting Information.

The physical and chemical properties of column effluent and released particles were characterized using ICP-AES, CVAFS, TEM, EXAFS spectroscopy, powder XRD, and sequential chemical extraction as described above. Concentrations of Al, Fe, Si, P, Ti, and S in column effluent samples were determined using an ICP-AES. Effluent samples were digested in HCl acid (trace metal grade) prior to analysis. To ensure complete digestion, a 1-mL aliquot of column effluent was digested overnight in 4.5 mL of concentrated HCl and then diluted to 10 mL with DI water. To distinguish between particulate and dissolved species, some samples were filtered (prior to acid digestion with HCl) using a 0.45-μm membrane or a 0.02-μm alumina matrix syringe filter. The finer filter (0.02 μm) was used in some cases to ensure that no particles (d_p > 20 nm) existed in the column effluent. Hence, the operational definition of "dissolved" in this work is any constituent finer than ∼20 nm in diameter rather the ∼450 nm that is commonly used.

The Hg concentration of the filtered or unfiltered column effluent samples was measured either by Frontier Geosciences (Seattle, WA) or at the University of Nevada, Reno (UNR). For analysis at Frontier, column effluent samples were preserved using a 50% (v/v) bromine monochloride solution, and an aliquot of each preserved sample was analyzed by $SnCl_2$ reduction, dual gold amalgamation, and CVAFS detection according to EPA method 1631. The estimated method detection limit was ∼3 ng/L. For analyses at UNR, filtered and unfiltered column effluents were analyzed using TDA/CVAFS according to EPA method 7473. The detection limit for Hg using this method was 1 μg/L.

Results and Discussion

Characterization of NI and SB Mercury Mine Tailings. The mineralogical and chemical compositions and size distributions of the NI and SB mine tailings are given in Table 1 and Supporting Information, respectively. A broad hump in the XRD patterns of the SB samples between 15 and 35° 2θ indicate an amorphous phase is present in addition to the crystalline phases. The primary matrix minerals in each tailings sample reflect the different geologic setting of each mine site. Differences in the primary matrix minerals between the SB calcines and waste rock are likely due to high-temperature ore processing. For example, cinnabar (HgS) would be largely removed from the ore material during processing and iron sulfide may have been oxidized to hematite during the roasting process.

The relative Hg concentration ($[Hg]_t/[Hg]_{max}$) as a function of particle size for each split is given in Figure 1. A clear trend exists for NI and SB calcines of increasing $[Hg]_t$ with decreasing particle size, which is consistent with those observed for mine tailings from different mines (*11*). The trend is consistent with that expected for adsorbed Hg, i.e., increasing $[Hg]_t$ concentration with increasing surface-area-to-volume ratio, which is a common conceptual model for heavy metal speciation in the environment (*33*, *34*). However some deviation from the expected trend exists (Figure 1). The Hg enrichment with decreasing particle size has been attributed to the relatively low hardness (H = 2.5) and solubility (K_{sp} values in the range of 10^{-36}) of the Hg-sulfide minerals cinnabar and metacinnabar (*11*). Hg may therefore be more prevalent in the smaller size fractions due to the accelerated physical weathering of HgS relative to the harder minerals present (e.g., quartz, H = 7). SB waste rock has significantly higher $[Hg]_T$ (1 to 2 orders of magnitude greater) than either of the calcines because this material was not processed to remove Hg. Unlike the SB and NI calcine

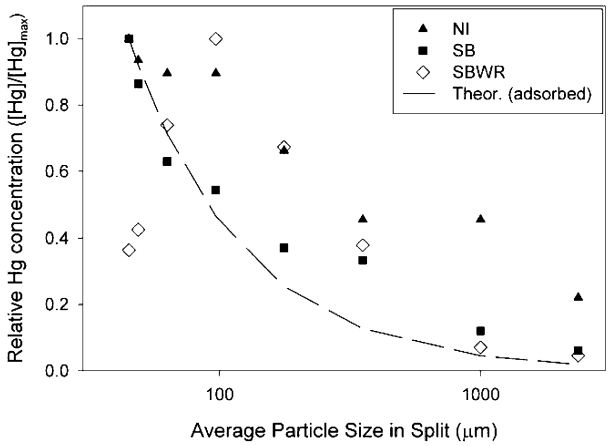

FIGURE 1. Relationship between particle size and $[Hg]_t$ for NI and SB calcines, and SB waste rock splits. Line represents expected trend for adsorbed Hg assuming spherical nonporous particles with the average diameter of that measured for the tailings.

materials, $[Hg]_T$ in SB waste rock did not increase with decreasing particle size, but instead reached a maximum (~22 000 mg/kg) at an intermediate particle size (125 μm > d_p > 75 μm). This phenomenon may reflect the Hg-mineral grain size distribution at the time of deposition. Differences between SB waste rock and calcines (i.e., higher $[Hg]_T$ and the presence of a $[Hg]_T$ maximum at an intermediate particle size), indicate that high-temperature ore processing (600−700 °C) affected the Hg distribution in the ore material in addition to extracting Hg.

SEM analysis (not shown) of NI and SB calcines (2−5 mm fraction) indicates the surfaces of the larger particles are covered with finer-grained particles adhered to the surface, ranging in size from 100 nm to several micrometers. The NI calcines showed the highest density of small particles adhered to surfaces, followed by the SB waste rock, then the SB calcines. EDX analyses of the NI calcines indicate that Al, Si, Fe, S, and P are the major elemental components of the surface particles, consistent with the chemical data and bulk matrix mineral components determined by XRD. EDX analyses of the SB materials indicates that the composition of the surface-bound particles on the SB calcines (Si, Al, S, and Fe) and SB waste rock (Si, Al, S, Fe, and Ti) are also consistent with the bulk matrix mineral components determined by XRD.

TEM analysis of the <45 μm NI calcines sieve fraction (Figure 2a) show μm and sub-μm-sized aggregates of fine-grained particles. EDX analysis identified the dominant components as hematite and alunite-jarosite and amorphous Al−Si material, consistent with the XRD results for the NI calcines (Table 1). Discrete sub-μm HgS particles (cinnabar or metacinnabar) were identified in some aggregates. TEM/EDX analysis of the < 45 μm SB calcine material (Figure 2b) correlates well with the XRD results indicating the presence of SiO_2 (quartz or cristobalite), hematite, anatase, and a poorly ordered Al−Si−Fe rich clay phase. Also present are euhedral particles containing Fe, S, and Al which may be alunite-jarosite. TEM/EDX analysis of the SB waste rock material (Figure 2c) indicates the presence of silica (quartz/cristobalite), anatase, and FeS (mackinawite) which is consistent with the XRD data for this material. Because the waste rock material contains high $[Hg]_T$, it was possible to observe discrete cinnabar particles (~500 nm) (Figure 2c). EDX confirmed the HgS chemical composition of these particles, and electron diffraction revealed the hexagonal symmetry of cinnabar (not shown).

Hg speciation in the NI and SB tailings, determined by Hg-EXAFS spectroscopy on three size fractions of each bulk

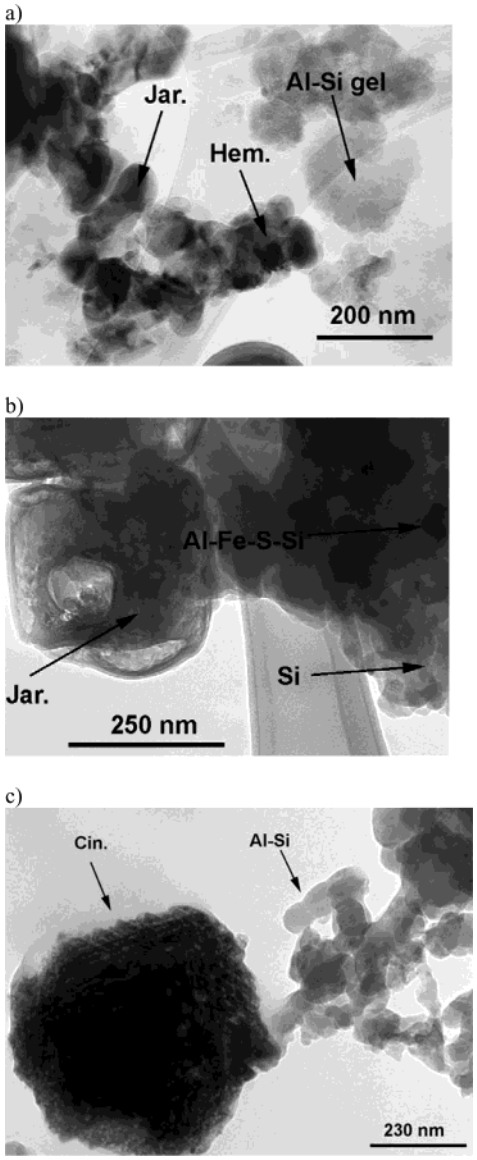

FIGURE 2. TEM micrographs of NI and SB calcines, and SB waste rock (d_p < 45 μm size fraction): (a) NI calcines, (b) SB calcines, and (c) SB waste rock.

material, are provided in Table 1. For the NI calcines, most of the Hg exists as Hg-sulfides (cinnabar/metacinnabar) and Hg-oxides (montroydite), but minor Hg-oxychloride (eglestonite) is also present. This is consistent with other studies of the Hg mineralogy at mine sites in the New Idria mining district (*35*). For the SB calcines and waste rock, nearly all the Hg is present as Hg-sulfide species. No evidence of sorbed Hg was found in any of the samples.

Results from the sequential extractions on both the pre- and postcolumn material of all three samples are shown in Figure 3. The F5 and F6 extraction steps, which dissolve HgS (both cinnabar and metacinnabar), remove the majority of Hg from all samples, accounting for 54.9−97.5% of all Hg removed and indicating that HgS constitutes the bulk of Hg present in both the pre- and postcolumn materials. Furthermore, the proportions of Hg removed in the F5 and F6 extraction steps of the precolumn material generally match well with the proportions of HgS identified in the same material by EXAFS spectroscopy, (e.g., 85.9% F5 + F6 removable vs 89% HgS for SB calcines, 95.5% vs 100% for SB waste rock), providing good consistency between the two techniques as previously observed (*32*). A moderate discrepancy was found between the two techniques for the NI

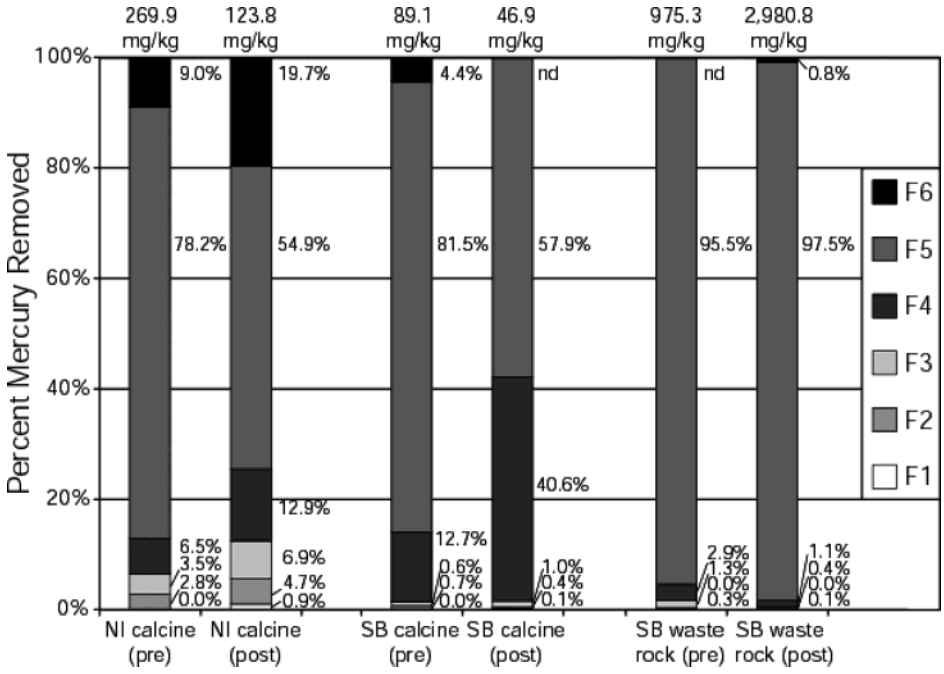

FIGURE 3. Sequential selective chemical extraction results on pre- and postcolumn material for the NI calcine, SB calcine, and SB waste rock, in descending order of extraction intensity (extractions are described in Table 3). Total extracted Hg is listed at the top of each column in mg/kg.

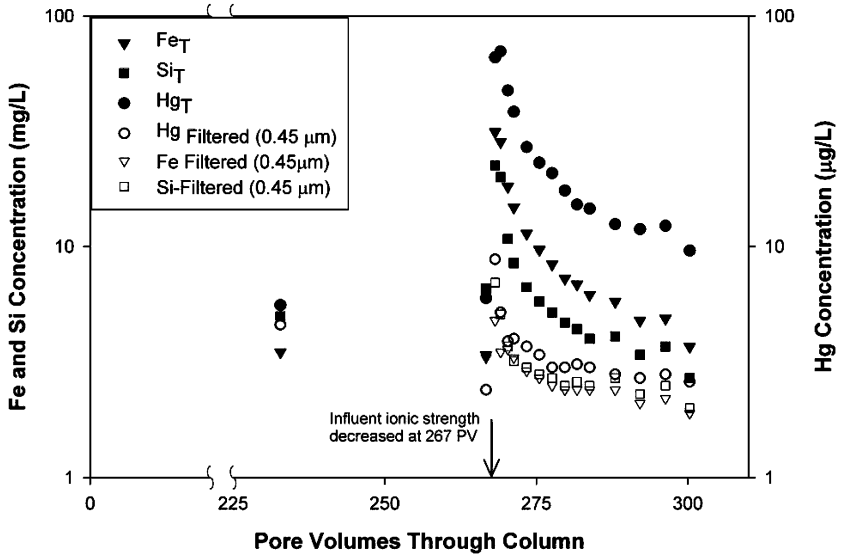

FIGURE 4. Concentrations of Fe, Si, and Hg in NI1 column effluent.

calcine (87.9% F5 + F6 removable vs 56% HgS from EXAFS spectroscopy). However, both methods are consistent in showing that the NI calcine has the lowest proportion of HgS among the three samples.

Analysis of both the pre- and postcolumn material for each sample reveals a decline in the total amount of Hg as well as the proportion of F5 + F6 removable Hg (i.e., HgS) in the calcines as a result of the column experiments (Figure 3), suggesting the release of HgS from the column material. Extraction results for the SB waste rock, however, are essentially unchanged between the pre-and postcolumn material due to the singular presence of HgS in the unroasted wastes (as confirmed by EXAFS spectroscopy). Additionally, $[Hg]_T$ in the postcolumn SB waste rock material is higher than that of the precolumn material, which is likely due to sample heterogeneity. Sample heterogeneity is more likely in the waste rock, compared to the calcines, because large HgS particles will have not been removed by calcination.

Particle/Hg Release from NI Mine Tailings. Effluent concentrations for selected elements during the preconditioning and particle release steps of the column experiments using NI calcines are given in Figure 4. The initial experiment run on the tailing with no malonic acid present released no particulate material and is therefore not considered in this study. The second preconditioning resulted in steady-state effluent concentrations less than 6 mg/L for Fe, Al, Si, S, and P, and less than 6 μg/L for Hg in unfiltered samples. Filtered samples (0.45-μm filter) showed concentrations similar or identical to those of unfiltered samples for each element, indicating that the elements exist as dissolved species or at least as dissolved species according to the common operational definition (passing through a 0.45-μm filter). Following the reduction of the ionic strength there is a large increase in the unfiltered concentration for all the elements, including Hg, with only a minor increase in the filtered concentrations. This indicates the release of particles from the column

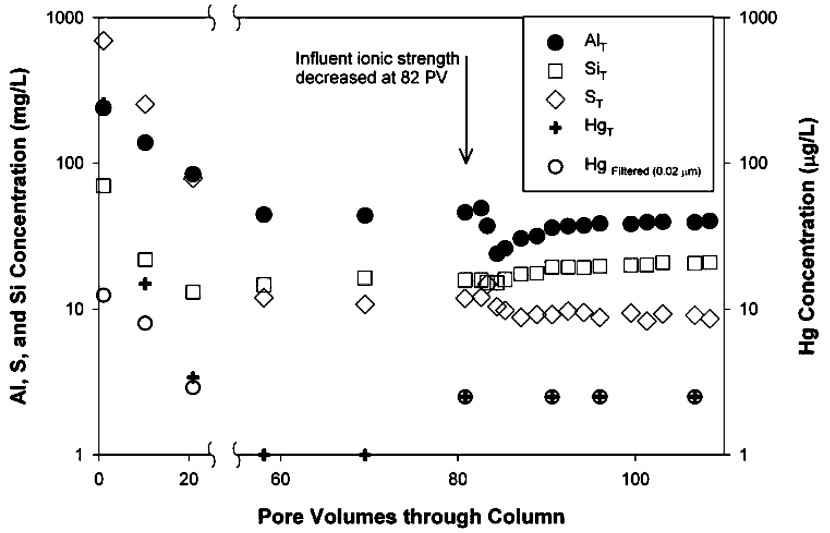

FIGURE 5. Concentrations of Al, Si, S, and Hg in SB calcines column effluent.

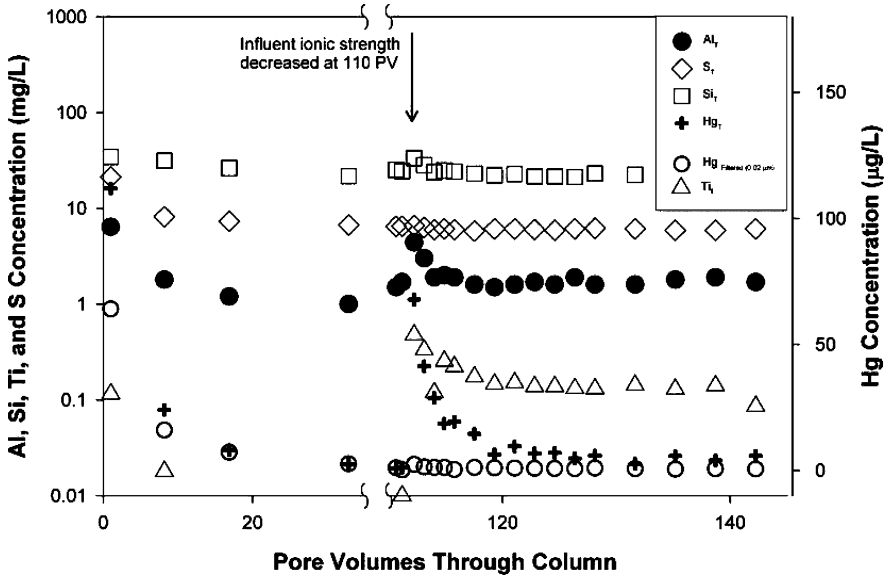

FIGURE 6. Concentrations of Al, Fe, Si, S, Ti, and Hg in SB waste rock column effluent.

material. Peak particle density occurred in the column effluent after one pore volume followed by a sustained release over at least 25 pore volumes. This type of decay in particle density (a sharp peak followed by slower release over many pore volumes) has been observed in other particle release experiments (*1*, *19*). The concentrations of Hg, Fe, and Si in filtered (0.45-μm) effluent samples were significantly lower than those for unfiltered samples, indicating that they are particle-associated during this phase. Other elements (not shown for clarity) showed identical trends.

The second column experiment (NI2) run on a separate set of NI calcines with the larger ionic strength drop showed an increased particle release as evidenced by a 5-fold increase in total unfiltered Fe and Al concentrations in effluent samples, a maximum unfiltered Hg concentration of 2000 μg/L, and visually more turbid column effluent during the particle release stage (Figure 1 Supporting Information). This behavior is consistent with particle release from silica sands (*19*) and noncalcareous soil aggregates (*16*), and has been attributed to a reduction in the energy barrier for particle release at lower ionic strength. The presence of the malonic acid also influenced the rate and quantity of particles released, as fewer particles were observed without it being present during preconditioning and particle release. Organic acids such as oxalic and malonic acid (dicarboxylic acids) can promote release of particles from aquifer material by initiating dissolution of the iron-(oxy)hydroxide cementing agent and by adsorbing to minerals and changing their surface charge such that the particles are easily released when their surrounding electric double layer size is increased due to the ionic strength decrease (*10*). It is likely that malonic acid increases the particle release rate without substantially altering the chemical composition of the released particles.

ATEM and XRD analyses of the colloids released from the NI tailings showed the presence of hematite (Fe_2O_3), jarosite/alunite ($(Fe,Al)KSO_4$), quartz (SiO_2), a poorly ordered Al−Si−Fe phase (Figure 7a), and HgS. The hematite crystallites are subhedral with a particle size of ~100 nm. EDX analysis indicates that the hematite is relatively pure with little or no Si or Al. Jarosite/alunite tends to be present as sub-euhedral crystals with particle sizes of 100−200 nm. The powder XRD pattern of the colloids has a peak at ~10Å, suggesting the presence of illite (*36*). Also, a poorly ordered Al−Si−Fe-rich phase was observed via TEM and consists of either sheetlike particles or aggregates of rounded particles <10-nm in diameter (Figure 7a). An average principle cation ratio of $Al_{0.30}Si_{0.66}Fe_{0.04}$ was determined using EDX analysis, indicating a (Al + Fe)/Si ratio ≈ 0.5. The diffraction and chemical data

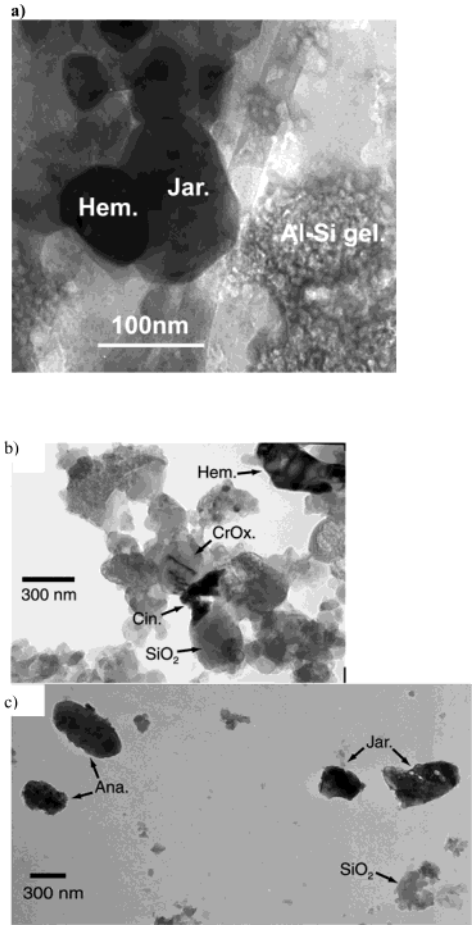

FIGURE 7. (a) TEM micrograph of colloids from the NI calcines column effluent produced during the particle release step. Note that the aluminosilicate gel consists of aggregates of particles <10 nm (Hem., hematite; Jar., jarosite; and Al−Si gel, aluminosilicate gel). (b) Colloids generated from the preconditioning and (c) particle release steps of the SB waste rock column experiment (Hem., hematite; CrOx, Cr-(hyr)oxide; Cin., cinnabar; SiO_2, silica; Ana, anatase; and Jar., Jarosite).

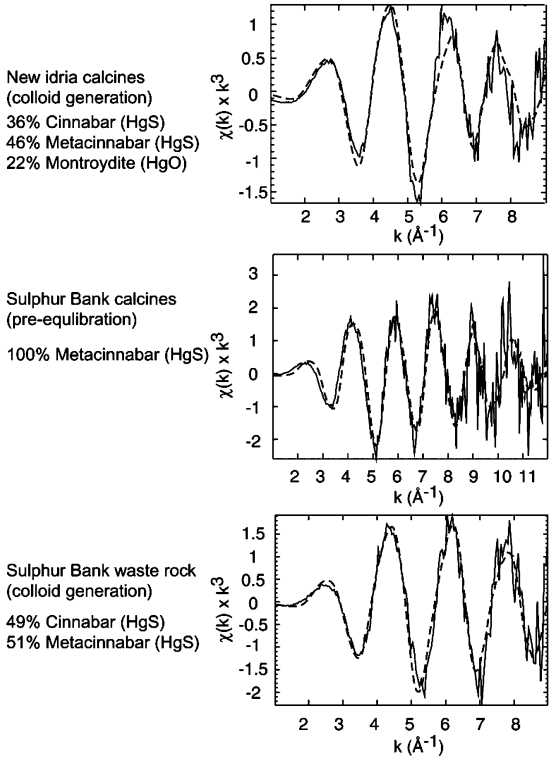

FIGURE 8. Liner fits of the Hg L_{III}-edge data for the NI and SB column effluent colloids. Quantitative compositions have an error of approximately ±10%. Black line, experimental data; dashed line, calculated fits.

suggest that this material is probably poorly ordered illite. Cinnabar is present at a concentration lower than that detectable by XRD (< ~5 wt %), but a small particle of cinnabar (44 nm diameter) was found using TEM. No other Hg-containing phases were observed via TEM or XRD. Hg-EXAFS analysis indicates that Hg is present dominantly as cinnabar or metacinnabar, with a lesser amount of montroydite (HgO) (Figure 8). Results from the sequential chemical extraction experiments indicate that significant amounts of Hg are removed in the 1 M HNO_3, 1 M KOH, and 12 M HNO_3 extraction steps (Table 2).

Particle/Hg Release from SB Calcines. Particle release from SB calcines was negligible relative to particle release from the NI calcines. Even though few observable particles were released from the SB calcines, high concentrations of Al, Si, and S were detected in the column effluent during preconditioning, decreasing slowly during the preconditioning phase, and reaching a steady state after approximately 60 pore volumes (Figure 5). The high Al, Si, and S concentrations relative to those in the NI calcines are due of differences in the mineralogy of the tailings at the two sites. Filtering the column samples (0.02 μm) did not reduce the concentrations of these species, suggesting they are truly dissolved.

Hg release from the SB calcines occurs primarily during preconditioning, with unfiltered Hg concentration in the column effluent decreasing rapidly from 260 μg/L to 3.4 μg/L after 21 pore volumes. Unlike Al, Si, and S, the Hg concentration was significantly reduced by filtering (0.02 μm) the column effluent, suggesting that the initial Hg release is predominantly particulate (colloidal), but that sustained low concentration Hg release occurs predominantly as dissolved species.

Reducing the ionic strength of the column influent did not initiate release of observable particles from the SB calcines or significantly increase the effluent Hg concentration. Instead, lowering the ionic strength resulted in a decrease in the dissolved Al, S, and Si concentrations (Figure 5). At the lower ionic strength, the activity coefficients of Al, S, and Si in solution decreases, lowering their solubility (*37*, *38*). Filtering (0.02 μm) did not reduce the S, Al, Si, and Fe concentrations, supporting the conclusion that few particles were released.

Colloidal particles released during the first few pore volumes of the preconditioning step were analyzed by TEM. Too few colloids were generated for XRD analysis. Only poorly ordered Al−Si gel and cinnabar were found in significant quantities using TEM. The Al−Si gel occurs as rounded agglomerates of approximately 200 nm with an Al/Si ratio of between 2 and 20 determined from EDX analysis. Fine structure within the individual aggregates indicates that they are an agglomerate of smaller particles (<10 nm). HgS occurs as subhedral crystallites of 200−400 nm. The Hg-EXAFS data confirms that Hg is present entirely as HgS (metacinnabar) (Figure 8).

Due to the large concentration of dissolved Si, Al, and Fe in solution (up to 341 ppm), a white precipitate formed when 1 M NaOH was added to the column effluent, up to pH 8. TEM analysis of the freeze-dried precipitate showed it to be a poorly ordered Al−Si−Fe gel consisting of aggregates of particles 3−4 nm in size (Figure 9a and c). The composition of the gel is uniform with a relative cation composition of $Al_{0.73}Si_{0.23}Fe_{0.0}$. XRD showed two broad diffraction peaks at

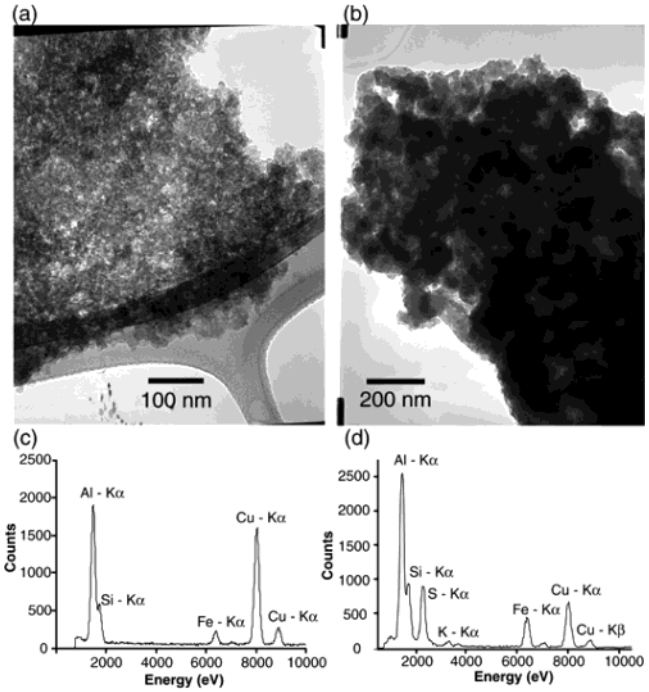

FIGURE 9. TEM micrograph of (a) Hg-doped Al−Si−Fe gel formed by the neutralization of the SB calcines column effluent and (b) natural Al−Si−Fe−S gel collected from the shore of Clear Lake next to the SB mine. EDX spectra of (c) Hg-doped Al−Si−Fe gel and (d) natural Al−Si−Fe−S gel. Note that peaks for Cu are contamination from the Cu grid.

6.1 and 3.2 Å, which correlate with the two most intense diffraction peaks for boehmite (γ-AlOOH). The diffuse nature of the Bragg peaks and the fine particle size of the precipitate indicate that this phase is psuedo-boehmite rather than boehmite (*39*). The presence of diffraction peaks for psuedo-boemite is probably related to particles of γ-AlOOH within the gel. Figure 9b shows a TEM micrograph of the natural SB flocculent material collected from the Clear Lake shoreline near the SB mine. It consists almost entirely of aggregates of <10 nm similar to the synthetic precipitate. The natural gel has a composition similar to that of the laboratory-generated floc but has a significant amount of sulfur (Figure 9d). XRD of the freeze-dried natural gel indicated the presence of crystalline quartz and halloysite ($Al_2Si_2O_5(OH)_4$), although the majority of the material is poorly ordered. This composition is similar to that observed by Suchanek et al. (*40*) for this material using SEM and ICP-MS.

ICP-AES analysis of the filtered supernatant from the $Hg(NO_3)_2$/SB calcines column effluent coprecipitate indicates that only 6% of the Hg added to the solution is associated with the gel and that 94% remains in solution. This low level of sorption is probably related to the relatively low Al, Si, and Fe content of the solution (Σ(Al,Si,Fe) = 341 mg/kg) which precipitate to form the floc. EXAFS results for the Hg-doped precipitate are shown in Figure 10 and Table 3, indicating that Hg(II) is coordinated by two oxygen shells. The Hg−O distances of these shells are close to those for oxygens surrounding Hg in crystalline montroydite (HgO) (*41*) (Table 3). The coordination number for the first shell is in close agreement with that for montroydite, but that of the second shell (1.6 oxygens) is considerably lower than found in montroydite (*41*). This result is almost identical to that of another Hg-EXAFS study of pure montroydite (*42*) and is likely affected by the uncertainties associated with EXAFS-derived coordination numbers (*N*) for distorted coordination environments such as Hg(II). Therefore, it is likely that the real *N* value for the second shell is closer to four.

Particle/Hg Release from SB Waste Rock. Concentrations of S, Al, Si, Ti, and Hg in effluent from the column containing SB waste rock are shown in Figure 6. The concentrations of

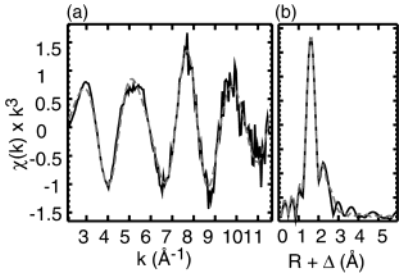

FIGURE 10. (a) Hg-L_{III} edge XAFS spectra of Hg-doped aluminosilicate gel precipitated from the SB calcines column effluent. (b) Fourier transform of the XAFS spectra uncorrected for phase shifts. Black line, experimental data; gray line, calculated fit.

TABLE 3. Structural Parameters Obtained From Nonlinear Least-Squares Fitting of the EXAFS for Hg Sorbed to the Synthetic Al−Si Gel Precipitated from the SB Calcines Column Effluent[a]

	Sulphur Bank Al−Si gel			montroydite	
	N	*R* (Å)	σ^2 (Å^2)	*N* ($HgO_{mont.}$)	*R* (Å) ($HgO_{mont.}$)
Hg−O	1.9	2.08	0.0057	2	2.05
Hg−O	1.6	2.95	0.013	4	2.83

[a] Also quoted are data for the local environment of mercury in montroydite (HgO) (*41*). *N* is the coordination number, *R* is the mercury-scatterer distance, and σ^2 is the Debye−Waller factor. The least squares errors (1s) associated with the EXAFS-derived *N*, *R*, and Debye−Waller factors are ±0.5 atoms, ±0.005 Å, and ±0.001 Å^2, respectively.

S, Al, and Si show a trend with pore volume similar to that of the SB and NI calcines, with concentrations decreasing slowly during the preconditioning phase and reaching a steady state. Additionally, Ti was released during preconditioning. The initial and steady-state effluent concentrations of most elements are more than an order of magnitude lower for the SB waste rock (Si was relatively unchanged) than the SB calcines. The time required to reach the steady-state effluent concentrations of each element was less for the SB

waste rock than the SB calcines, and the relative concentrations of Al, S, and Si in effluent samples were different. This is probably related to differences in mineralogy and chemical composition between the two mine waste materials. Hg release from the SB waste rock during preconditioning showed a similar trend to Hg release from the SB calcines, with most Hg release occurring in the first 20 pore volumes. Similar to the SB calcines, filtering (0.02 μm) did not affect Al, Si, S, and Fe concentrations, but did lower Ti and Hg concentrations by 40−50% in the first two samples. By the end of preconditioning, filtering had no impact on Ti and Hg concentration. This suggests that the initial Hg release is dominantly particle-associated Hg (perhaps Ti particles), but sustained Hg release occurs as dissolved species or as particulate Hg less than 0.02 μm.

Lowering the column influent ionic strength resulted in particle release as evidenced by an increase in Si, Al, S, and Ti concentrations, but the particle density was significantly lower than that for the NI calcines. As with NI calcines, the increase in the unfiltered Hg concentration in column effluent was coincident with particle release, indicating the two processes are related. Filtering the effluent samples (0.02 μm) did not reduce Al, Si, or S concentrations, indicating these elements exist predominantly as dissolved species. However, filtering (0.02 μm) did decrease the $[Hg]_T$ and Ti concentration by 80−96% and 75−96%, respectively, during particle release. A clear trend existed, with particle-associated Hg accounting for 96% of Hg released at the onset of particle release, and decreasing to 80% at the end of particle release. It is unclear why filtration affects Ti and Hg concentrations, but not the concentrations of other elements present. It is possible that the concentrations of dissolved Al, Si, and S are high enough to mask the contribution of particles to the total concentration for these elements. This is not the case for Hg and Ti, and therefore the effect of filtration (particle removal) is more pronounced.

Colloids generated during the first few pore volumes of the preconditioning step were very heterogeneous. The major phases observed using TEM were HgS, Cr−(oxyhydr)oxide, Al−Si gel, hematite, silica, and Fe-sulfide (Figure 7b), all of which are <500 nm in size. The crystalline polymorphs of Cr−(oxyhyr)oxide, silica, and Fe-sulfide cannot be determined unequivocally due to their small particle size and electron beam sensitivity. However, the mineralogical composition of the waste rock starting material suggests that the silica mineral is cristobalite and the Fe-sulfide phase is mackinawite, suggesting that the colloids are formed by breakup of the waste rock. The colloids generated following the lowering of the influent ionic strength are significantly different from those released during the preconditioning step. The major phases observed using TEM are HgS, Ti-oxide, jarosite/alunite, and silica (Figure 7c). XRD analysis of the waste rock starting material indicates the silica polymorph is cristobalite and the Ti-oxide polymorph is anatase. Anatase is present as anhedral sub-angular particles of up to 1 μm, although these large particles may be agglomerates of smaller grains (Figure 7c). The cristobalite and jarosite particles are also anhedral and sub-angular with sizes up to 1 μm. HgS grains are up to 500 nm, but many are <50 nm. EXAFS analysis of the colloids released (Figure 8) supports the TEM observations and indicates that EXAFS-observable Hg is entirely in the HgS form, with an approximate 50:50 mixture of cinnabar and metacinnabar.

Origin and Nature of Colloids Released from New Idria and Sulphur Bank Mine Waste. The variation in composition of the colloids is directly related to the composition of the starting material from which the colloids are generated. All of the released colloids appear to have formed via detachment and breakup of the bulk mine waste. This is indicated by the similarity in composition of the Hg-phases in the colloids to those in the mine wastes, the only difference being the lack of any soluble mercury phases (i.e., $HgCl_2$), which are probably leached out during preconditioning. The dissolved Hg produced by the dissolution of the soluble Hg-phases could have produced a high concentration of sorbed Hg, but none was detected in the SB calcines preconditioning colloids. The reason is probably related to the relatively low concentration of sorbed mercury relative to HgS in the colloid.

The composition of the colloids varies according to whether they were released during the first few pore volumes of the experiments (preconditioning) or when the ionic strength of the influent solution was lowered (particle release). Colloids released during the preconditioning step relate to material poorly adhered to the surfaces of the larger particles in the column and could be weathering products on the outer surfaces of these particles (e.g., Al−Si gel/clay). The SB waste rock released the most colloidal material during preconditioning, which may be related to its lack of roasting. Such roasting can cause cementing of particles within larger grains due to recrystallization and melting that occurs at high temperature. There are also large variations in the crystallinity of different mineral colloids (e.g., ranging from amorphous Al−Si gel to fully crystalline hematite and jarosite). Crystallinity correlates with particle size, with the poorly ordered material having particle diameters of 10 to 50 nm and the fully crystalline phases having diameters generally above 200 nm, with some particles having diameters >1 μm. The poorly ordered gel and clay phases are probably secondary weathering products of the primary minerals that made up the calcines or waste rock. The reason for the lack of very fine crystalline phases in the colloids may be due to the fact that as particles get smaller, due to mechanical and chemical weathering, their solubility and dissolution rates increase (*43*, *44*). An exception to this generalization are crystalline mineral phases with very low solubility such as cinnabar ($HgS_{cin} + H^+ \leftrightarrow Hg^{2+} + HS^-, K = 10^{-36.7}$ (*45*)). The low solubility of HgS is thought to be the reason very-fine-grained HgS is present in the released colloidal material.

The similarity in composition and morphology of the Al−Si−Fe gel precipitated from the SB calcines column effluent and the natural floc found near the shore of Clear Lake near the SB mine indicates that the natural floc is likely formed by precipitation of an Al−Si−Fe-bearing phase, the components of which were leached from the calcines. No precipitates formed when the NI and SB waste rock column effluents were neutralized, indicating that this effect is specific to the SB calcines. Suchanek et al. (*40*) report that this floc material is a major source of methylmercury to Clear Lake. The reason for this high methylmercury concentration is not clear, but may be related to the high surface area of the floc.

It has been hypothesized that Hg can be transported in association with natural colloids as a sorbed species or as discrete particles (*8*, *9*). Our TEM and EXAFS results for the colloids generated from the SB calcines and waste rock indicate that Hg released from these mine waste materials is in the form of cinnabar or metacinnabar. TEM and EXAFS data from the NI colloids indicate that HgS is the dominant Hg phase, although the sequential extraction data do not fully agree with this finding. First, 33% of the Hg is extracted by 1 M HNO_3, which can be correlated with the presence of montroydite (HgO) and is within error the same as the fraction of this phase determined by XAFS spectroscopy (22%). The EXAFS data indicate that the remaining Hg in the colloid fraction is present as HgS. This finding contradicts the sequential extraction data, which indicate that 50% is removed by 12 N HNO_3 and 16% by aqua regia. Previous extraction studies on model compounds indicate that HgS is only dissolved during the aqua regia extraction; therefore, Hg extracted in the 12 N HNO_3 extraction step is not thought to be HgS (*46*). A more recent study has shown that fine-

grained metacinnabar is relatively soluble in 6 M HCl, and not just in aqua regia (*47*). There are two possible explanations for the discrepancy between the sequential extraction and EXAFS results discussed above: (1) the presence of another Hg-containing phase in the sample, or (2) the very fine particle size (<100 nm) of the HgS. The most likely candidate for another Hg-containing phase is elemental Hg, which cannot be easily detected by EXAFS, due to the lack of order in Hg^0 liquid, or TEM, because Hg^0 quickly volatilizes when placed in a vacuum. Concerning option (2), the solubility of solids increases exponentially with deceasing particle size at very small particle sizes (*43*, *48*), which may cause the nanoparticulate metacinnabar to have an increased solubility in 12 N HNO_3. If this is correct, the proportions of Hg extracted in the 12 N HNO_3 and aqua regia steps correlate qualitatively with the proportions of cinnabar and metacinnabar determined by EXAFS analysis.

The two main reasons for the domination of HgS in the colloids are the softness of the cinnabar and metacinnabar and their low solubility in water. These two factors lead to the persistence of fine-grained cinnabar in the near-surface aqueous environment. Therefore, nanometer-scale HgS particles are the dominant colloidal forms of Hg transported from these and other mine sites where cinnabar is the main solid Hg waste phase. No evidence was found for Hg sorbed to other colloidal mineral phases, in contrast to what has been suggested by other workers (*8*, *9*).

Implications for Hg Transport from Mine Sites. During episodic particle release due to a chemical perturbation particulate HgS is released from mine tailings and can be significant. Similar mechanisms are likely to occur at mines and should be considered in addition to conventional modes of Hg transport such as dissolved Hg and sorbed Hg(II) species. The significance of particle-facilitated Hg release and transport relative to dissolved Hg transport will depend on the ore type, ore processing, and environmental conditions at the site. In particular, the magnitude and frequency of the chemical perturbations at the site relative to steady flow conditions will dictate the relative contributions of each release mechanism. The release of particulate Hg is consistent with studies reporting the majority of Hg contamination exists as particle-associated or sediment-bound Hg (*49*−*52*).

Even though the particle release rate was enhanced in laboratory column studies relative to that expected under field conditions and therefore may overstate the quantity of particles released, the release of fine-grained particles (colloids) from mine wastes is likely. In fact, simply mixing NI calcines with DI water and shaking for several minutes resulted in the release of many fine-grained particles that remained suspended for several hours. TEM analysis of these colloids showed that the chemical composition and morphology were identical to those observed in the column experiments. Conditions at many mine sites may be conducive to particle release. Hg mine drainage with high ionic strength (4−12 g/L TDS) commonly flows through mine tailings at many Hg mines in the Coast Range mercury belt of California (*8*) and is similar to those used in the column experiments (0.1 M NaCl provides ∼5600 mg/L TDS). During the Winter wet season the TDS (i.e., ionic strength) of mine drainage is significantly diluted (by a factor of 6 or more), and colloids may be generated and transported from tailings previously exposed to high TDS mine drainage. This occurs at the Mount Diablo Hg mine for example and may account for the 2-fold increase in total and filterable Hg during the winter (*8*). At Hg mines without mine drainage, particle release may still occur when efflorescent salts are dissolved at the onset of the wet season and high ionic strength or high pH fluid flowing through tailings becomes progressively more dilute with additional rainfall.

Particulate Hg is expected to behave differently than dissolved Hg species in terms of transport and bioavailability. For example, surface and subsurface transport of dissolved Hg could be significantly retarded due to partitioning to noncolloidal solids as Hg has a relatively high effective distribution coefficient ($\log K_d \approx 4-6$) (*53*). Surface and subsurface transport of stable particulate Hg species (e.g., HgS) would be less retarded, particularly if particles are in the colloidal size range.

The extent and speciation of Hg released from mine wastes was different for different primary ores (Si-carbonate vs hot spring) and depended on whether the ore had been processed (calcined). For example, SB calcines released few particles and no particulate Hg, but unprocessed SB waste rock did release particles and primarily particulate Hg. Moreover, during particle release episodes the mass of Hg released from SB waste rock was lower than that from NI calcines, despite the higher Hg content in the starting material. This study is a first step at better understanding the factors affecting Hg release from mine wastes. Determining the speciation of released Hg provides a more thorough scientific basis for regulatory decisions, as opposed to relying exclusively on $[Hg]_T$.

Acknowledgments

This research was supported by the U.S. Environmental Protection Agency's EPA-STAR program (R827634), the U.S. Geological Survey, Geologic Division, and the National Center for Electron Microscopy (Grant 594). Although the research described in this article has been funded in part by the U.S. EPA, it has not been subject to EPA's required peer and policy review and therefore does not necessarily reflect the views of EPA, and no official endorsement should be inferred. We thank Dr. Daniel Grolimund (Swiss Light Source, Villingen, Switzerland) for help designing the column experiments, Prof. Mae Gustin (University of Nevada, Reno) for providing Hg analyses of column effluent, Bob Jones (Stanford University) for assisting in SEM and XRD analysis, Chuck Echer and Kandi Rodriguez (LBNL) for assisting in the ATEM analysis, and Dr. Nicholas Bloom (Frontier Geosciences) for performing the sequential extraction analyses. SSRL is supported by the Department of Energy (BES and BER) and the National Institutes of Health.

Supporting Information Available

Concentrations of Hg and select elements in nine different size fractions of the New Idria and Sulphur Bank mercury mine wastes; physical properties of each column test; figure showing colloid suspensions in NI2 column effluent ranging from 0 to 20 pore volumes through the column. This material is available free of charge via the Internet at http://pubs.acs.org.

Literature Cited

(1) Grolimund, D.; Borkovec, M.; Barmettler, K.; Sticher, H. Colloid-Facilitated Transport of Strongly Sorbing Contaminants in Natural Porous Media: A Laboratory Column Study. *Environ. Sci. Technol.* **1996**, *30*, 3118−3123.

(2) Roy, S. B.; Dzombak, D. A. Sorption nonequilibrium effects on colloid-enhanced transport of hydrophobic organic compounds in porous media. *J. Contam. Hydrol.* **1998**, *30*, 179−200.

(3) McCarthy, J. F.; Zachara, J. M. Subsurface Transport of Contaminants: Mobile Colloids in the Subsurface Environment May Alter the Transport of Contaminants. *Environ. Sci. Technol.* **1989**, *23*, 496−502.

(4) Kersting, A. B.; Efurd, D. W.; Finnegant, D. L.; Rokop, D. J.; Smith, D. K.; Thompson, J. L. Migration of Plutonium in Ground Water at the Nevada Test Site. *Nature* **1999**, *397*, 56−59.

(5) Ryan, J. N.; Elimelech, M. Colloid mobilization and transport in groundwater. *Colloids Surf. A* **1996**, *107*, 1−56.

(6) Puls, R. W.; Powell, R. M. Transport of Inorganic Colloids Through Natural Aquifer Material: Implications for Contaminant Transport. *Environ. Sci. Technol.* **1992**, *26*, 614−621.
(7) Elimelech, M.; Ryan, J. N. In *Interaction Between Soil Particles and Microorganisms*; Senesi, N., Ed.; John Wiley & Sons: New York, 2002.
(8) Rytuba, J. J. Mercury Mine Drainage and Processes that Control its Environmental Impact. *Sci. Total Environ.* **2000**, *260*, 57−71.
(9) Ganguli, P. M.; Mason, R. P.; Abu-Saba, K. E.; Anderson, R. S.; Flegal, A. R. Mercury Speciation in Drainage from the New Idria Mercury Mine, California. *Environ. Sci. Technol.* **2000**, *34*, 4773−4779.
(10) Swartz, C. H.; Gschwend, P. M. Mechanisms Controlling Release of Colloids to Groundwater in a Southeastern Coastal Plain Aquifer Sand. *Environ. Sci. Technol.* **1998**, *32*, 1779−1785.
(11) Kim, C. S.; Rytuba, J. J.; Brown, G. E., Jr. Geologic and anthropogenic factors influencing Hg speciation in mine wastes: an EXAFS spectroscopy study. *Appl. Geochem.* **2004**, *19*, 379−393.
(12) Benoit, J. M.; Gilmour, C. C.; Mason, R. P.; Heyes, A. Sulfide Controls on Mercury Speciation and Bioavailability to Methylating Bacteria in Sediment Pore Waters. *Environ. Sci. Technol.* **1999**, *33*, 951−957.
(13) Benoit, J. M.; Gilmour, C. C.; Mason, R. P. The Influence of Sulfide on Solid-Phase Mercury Bioavailability for Methylation by Pure Cultures of *Desulfobulbus propionicus* (1pr3). *Environ. Sci. Technol.* **2001**, *35*, 127−132.
(14) Farrell, R. E.; Huang, P. M.; Germida, J. J. Biomethylation of Mercury(II) Adsorbed on Mineral Colloids Common in Freshwater Sediments. *Appl. Organomet. Chem.* **1998**, *12*, 613−620.
(15) Swartz, C. H.; Gschwend, P. M. Hydrogeochemistry and Water Chemistry − Field studies of in situ colloid mobilization in a Southeastern Coastal Plain Aquifer. *Water Resour.s Res.* **1999**, *35*, 2213−2223.
(16) Grolimund, D.; Borkovec, M. Long-Term Release Kinetics of Colloidal Particles from Natural Porous Media. *Environ. Sci. Technol.* **1999**, *33*, 3, 4054−4060.
(17) Bunn, R. A.; Magelky, R. D.; Ryan, J. N.; Elimelech, M. Mobilization of Natural Colloids from an Iron Oxide-Coated Sand Aquifer: Effect of pH and Ionic Strength. *Environ. Sci. Technol.* **2002**, *36*, 314−322.
(18) Flury, M.; Mathison, J. B.; Harsh, J. B. In Situ Mobilization of Colloids and Transport of Cesium in Hanford Sediments. *Environ. Sci. Technol.* **2002**, *36*, 5335−5341.
(19) Roy, S. B.; Dzombak, D. A. Colloid release and transport processes in natural and model porous media. *Colloids Surf., A* **1996**, *107*, 245−262.
(20) Kaplan, D. I.; Bertsch, P. M.; Adriano, D. C. Facilitated Transport of Contaminant Metals Through an Acidified Aquifer. *Ground Water* **1995**, *33*, 708−717.
(21) Seaman, J. C.; Bertsch, P. M.; Miller, W. P. Chemical Controls on Colloid Generation and Transport in a Sandy Aquifer. *Environ Sci. Technol.* **1995**, *29*, 1808−1815.
(22) Ryan, J. N.; Gschwend, P. M. Colloid mobilization in two Atlantic coastal plain aquifers: field studies. *Water Resour. Res.* **1990**, *26*, 307−322.
(23) Roy, S. B.; Dzombak, D. A. Chemical Factors Influencing Colloid-Facilitated Transport of Contaminants in Porous Media. *Environ. Sci. Technol.* **1997**, *31*, 656−664.
(24) Ryan, J.; Gschwend, P. Effects of Ionic Strength and Flow Rate on Colloid Release: Relating Kinetics to Intersurface Potential Energy. *J. Colloid Interface Sci.* **1994**, *164*, 21−34.
(25) Ryan, J. N.; Gschwend, P. M. Effect of Solution Chemistry on Clay Colloid Release from an Iron Oxide-Coated Aquifer Sand. *Environ. Sci. Technol.* **1994**, *28*, 1717−1726.
(26) Rytuba, J. J. In *Geology and Ore Deposits of the American Cordillera: Symposium Proceedings*; Coyner, A., Fahey, P., Eds.; Geological Society of Nevada: Reno, NV, 1996; pp 803−822.
(27) Boctor, N.; Shieh, Y.; Kullerud, G. Mercury ores from the New Idria mining district, California: geochemical and stable isotope studies. *Geochim. Cosmochim. Acta* **1987**, *51*, 1705−1715.
(28) Linn, R. K. New Idria Mining District. In *Ore Deposits of the United States, 1933-1967; the Graton-Sales Volume*; Ridge, J. D., Ed.; American Institute of Mining, Metallurgical, and Petroleum Engineers: New York, 1968.
(29) Kim, C. S.; Brown, J. G. E.; Rytuba, J. J. Characterization and Speciation of Mercury-bearing Mine Wastes using X-ray Absorption Spectroscopy. *Sci. Total Environ.* **2000**, *261*, 157−168.
(30) Kim, C. S.; Rytuba, J. J.; Brown, G. E., Jr. EXAFS study of Hg(II) sorption to Fe- and Al−(hydr)oxide surfaces: I. Effects of pH. *J. Colloid Interface Sci.* **2004**, *271*, 1−15.
(31) Kim, C. S.; Rytuba, J. J.; Brown, G. E., Jr. EXAFS study of Hg(II) sorption to Fe- and Al-(hydr)-oxide surfaces: II. Effects of chloride and sulfate. *J. Colloid Interface Sci.* **2004**, *270*, 9−15.
(32) Kim, C. S.; Bloom, N. S.; Rytuba, J. J.; Brown, G. E., Jr. Mercury Speciation by X-ray Absorption Fine Structure Spectroscopy and Sequential Chemical Extractions: A Comparison of Speciation Methods. *Environ. Sci. Technol.* **2003**, *37*, 5102−5108.
(33) Brook, E.; Moore, J. Particle-size and Chemical Control of Arsenic, Cadmium, Copper, Iron, Manganese, Nickel, Lead, and Zinc in Bed Sediments from the Clark Fork River, Montana (USA). *Sci. Total Environ.* **1988**, *76*, 247−266.
(34) Moore, J.; Brook, E.; Johns, C. Grain Size Partitioning of metals in contaminated, coarse-grained river floodplain sediment: Clark Fork River, Montana, USA. *Environ. Geol. Water Sci.* **1989**, *14*, 107−115.
(35) Roberts, A. C.; Paar, W. H.; Stanley, C. J.; Dunning, G. E.; Bums, P. C.; Cooper, M. A.; Hawthorne, F. C.; Stirling, J. A. R. *Vasilyevite, $(Hg_2)^{2+}$. Can. Mineral.* **2003**, *41*, 1167−1172.
(36) Velde, B. *Introduction to Clay Minerals: Chemistry, Origins, Uses and Environmental Significance*; Chapman and Hall: London, 1992.
(37) Stumm, W.; Morgan, J. J. *Aquatic Chemistry: An Introduction Emphasizing Chemical Equilibria in Natural Waters*, 2nd ed.; Wiley: New York, 1981.
(38) Krauskopf, K. B.; Bird, D. K. *Introduction to Geochemistry*, 3rd ed.; McGraw-Hill: New York, 1995.
(39) Tettenhorst, R.; Hofmann, D. A. Crystal-Chemistry of Boehmite. *Clays Clay Miner.* **1980**, *28*, 373−380.
(40) Suchanek, T. H.; Richerson, P. J.; Flanders, J. R.; Nelson, D. C.; Mullen, L. H.; Brister, L. L.; Becker, J. C. Monitoring inter-annual variability reveals sources of mercury contamination in Clear Lake, California. *Environ. Monit. Assess.* **2000**, *64*, 299−310.
(41) Aurivillius, K. Least-Squares Refinement of the Crystal Structures of Orthorhombic HgO and of Hg_2O_2NaI. *Acta Chem. Scand.* **1964**, *18*, 1305−1306.
(42) Collins, C. R.; Sherman, D. M.; Ragnarsdottir, K. V. Surface Complexation of Hg^{2+} on Goethite: Mechanism from EXAFS Spectroscopy and Density Functional Calculations. *J. Colloid Interface Sci.* **1999**, *219*, 345−350.
(43) Adamson, A. W. *Physical Chemistry of Surfaces*, 6th ed.; Wiley: New York, 1997.
(44) Enustun, B. V., Turkevich, J. Solubility of fine partilces of strontium sulfate. *J. Am. Chem. Soc.* **1960**, *82*, 4502−4509.
(45) Paquette, K.; Helz, G. Solubility of Cinnabar (Red Hgs) and Implications For Mercury Speciation in Sulfidic Waters. *Water, Air, Soil Pollut.* **1995**, *80*, 1053−1056.
(46) Martian-Doimeadios, R. C. R.; Wasserman, J. C.; Bernejo, L. F. G.; Amouroux, D.; Nevado, J. J. B.; Donard, O. F. X. Chemical availability of mercury in stream sediments from the Almadén area, Spain. *J. Environ. Monit.* **2000**, *4*, 360−366.
(47) Mikac, N.; Foucher, D.; Niessen, S.; Fischer, J. C. *Anal. Bioanal. Chem.* **2002**, *374*, 1028−1033.
(48) Enustun, B. V.; Turkevich, J. *J. Am. Chem. Soc.* **1960**, *82*, 4502−4509.
(49) Domagalski, J. Occurrence and transport of total mercury and methyl mercury in the Sacramento River basin, California. *J. Geochem. Explor.* **1998**, *64*, 277−291.
(50) Barnett, M. O.; Harris, L. A.; Turner, R. R.; Stevenson, R. J.; Henson, T. J.; Melton, R. C.; Hoffman, D. P. Formation of Mercuric Sulfide in Soil. *Environ. Sci. Technol.* **1997**, *31*, 3037−3043.
(51) Hurley, J. P.; Cowell, S. E.; Shafer, M. M.; Hughes, P. E. Partitioning and Transport of Total and Methyl Mercury in the Lower Fox River, Wisconsin. *Environ. Sci. Technol.* **1998**, *32*, 1424−1432.
(52) Roth, D. A.; Taylor, H. E.; Domagalski, J.; Dileanis, P.; Peart, D. B.; Antweiler, R. C.; Alpers, C. N. Distribution of inorganic mercury in Sacramento River water and suspended colloidal sediment material. *Arch. Environ. Contam. Toxicol.* **2001**, *40*, 161−172.
(53) Suchanek, T. H.; Mullen, L. H.; Lamphere, B. A.; Richerson, P. J.; Woodmansee, C. E.; Slotton, D. G.; Harner, E. J.; Woodward, L. A. Redistribution of mercury from contaminated lake sediments of Clear Lake, California. *Water, Air, Soil Pollut.* **1998**, *104*, 77−102.

Received for review June 20, 2003. Revised manuscript received July 19, 2004. Accepted July 20, 2004.

ES034636C